J. Fluid Mech. (2005), *vol.* 535, *pp.* 369–381.
doi:10.1017/S002211200500474X Printed in the United Kingdom

Effective viscosity of grease ice in linearized gravity waves

By G. DE CAROLIS[1], P. OLLA[2] AND L. PIGNAGNOLI[3,4]

[1]ISSIA-CNR, I–70126 Bari, Italy

[2]ISAC-CNR, Sez. Lecce, I–73100 Lecce, Italy

[3]ISAC-CNR, I–40129 Bologna, Italy

[4]Dipartimento di Matematica, Universitá di Milano, I–20133 Milano, Italy

(Received 11 February 2004 and in revised form 31 January 2005)

Grease ice is an agglomeration of disk-shaped ice crystals, named frazil ice, which forms in turbulent waters of the Polar Oceans and in rivers as well. It has been recognized that the property of grease ice that it damps surface gravity waves could be explained in terms of the effective viscosity of the ice slurry. This paper is devoted to the study of the dynamics of a suspension of disk-shaped particles in a gravity wave field. For dilute suspensions, depending on the strength and frequency of the external wave flow, two orientation regimes of the particles are predicted: a preferential orientation regime with the particles rotating in coherent fashion with the wave field, and a random orientation regime in which the particles oscillate around their initial orientation while diffusing under the effect of Brownian motion. For both motion regimes, the effective viscosity has been derived as a function of the wave frequency, wave amplitude and aspect ratio of the particles. Model predictions have been compared to wave attenuation data in frazil ice layers grown in wave tanks.

1. Introduction

Grease ice is a thin slurry of disk-like platelets of ice crystals, called frazil ice, which forms in supercooled waters of the Polar Oceans under cold and windy conditions. Frazil disks measure approximately 0.1–0.4 cm in diameter and 1–100 μm in thickness (Kivisild 1970). Grease ice can accumulate up to tens of centimetres thick and significantly affect ocean surface roughness by attenuating short waves. This effect has been widely documented by observations of early whalers. Furthermore, synthetic aperture radar imagery of grease ice appears dark because of the suppression of the gravity–capillary waves resonant with the incident microwave radiation (1–10 cm) (Wadhams & Holt 1991).

Laboratory measurements of wave propagation in grease ice show that wave attenuation can be explained in terms of the medium effective viscosity (Newyear & Martin 1997). Martin & Kauffman (1981) developed a viscous-plastic model to explain the observed wave attenuation. They claimed that the viscous nature of grease ice could arise from interactions among frazil crystals leading to the presence of an energy sink in the wave dynamics. The authors did not present any estimate of grease ice effective viscosity from their data. On the other hand, wave dispersion and attenuation data of Newyear & Martin (1997) were consistent with a constant viscosity value, comparable to that of glycerin at 0 °C, in the range of frequencies

from 6.6 to $9.5\,s^{-1}$ (Newyear & Martin 1999). The viscosity was estimated using a two-layer wave propagation model, which represents grease ice as a viscous fluid superimposed on inviscid water (Keller 1998).

The concept of bulk viscosity for grease ice holds because the size of the frazil particles (~ 0.1 cm) is much smaller than both the vertical scale of grease ice (10 cm in the laboratory) and the horizontal scale of the travelling wave (from $\sim$100 cm in the laboratory to hundreds of metres in the ocean) (Newyear & Martin 1999).

From the theoretical point of view, it is possible to obtain detailed information on the behaviour of a suspension of disk-like particles in the velocity field of a gravity wave only in the dilute limit. In this limit, the problem becomes that of the behaviour of an individual particle in a given flow field, in the absence of interactions with the other particles in suspension. Iterative approaches such as that of the differential scheme (Bruggeman 1935) can then be used to obtain semi-quantitative information in the high-volume-fraction regimes characteristic of grease ice.

A second simplification is obtained by disregarding inertia effects at the scale of the ice platelets. Starting from the work of Jeffery (1922), much effort has been devoted to the dynamics of an ellipsoidal particle under creeping flow conditions. The importance of Brownian motion for the presence of an equilibrium particle orientation distribution, and consequently for the existence of a uniquely defined bulk viscosity, was already recognized by Taylor (1923). It turns out that, unless the particles are so small that Brownian diffusion dominates, the external flow strongly influences the orientation distribution and this effect cannot be disregarded for relatively large particles like the ice platelets. As recognized by Bretherton (1962), this may lead, in flow regions characterized by high strain and low vorticity, to the possibility of fixed orientation regimes for the particles. Only more recently, however, have time-dependent situations involving ellipsoids in suspension, come under scrutiny. In Zhang & Stone (1998), the forces and torques acting on an oscillating disk in a quiescent fluid have been calculated. In Szeri, Milliken & Leal (1992), the orientation dynamics of an ellipsoidal particle under the effect of combined time-dependent vorticity and strain has been analysed.

The calculation of the bulk viscosity of a dilute suspension of ellipsoids in a plane shear was carried out in Leal & Hinch (1972), in the regime of small but non-zero Brownian motion. The effective viscosity of a concentrated suspension of aligned disks was studied in Sundararajakumar, Koch & Shaqfeh (1994), using slender body theory arguments. In Phan-Thien & Pham (2000), a differential scheme approach was used to calculate the effective viscosity in the concentrated regime assuming random orientation of the ellipsoids. In all cases a time-independent situation was considered.

In the present paper, we shall consider the case of gravity waves in infinitely deep water. In this case, it is possible to pass to a reference frame in which the flow is time independent, and this eliminates the possibility of irregular orbits in orientation space, as observed in Szeri *et al.* (1992) in the case of simple periodic flows.

This paper is organized as follows. In the next section, the orientation dynamics of a Stokesian particle in a deep-water gravity wave will be elucidated. In particular, the possibility of coherent collective motions in the suspension will be examined. In § 3, the effective viscosity of a dilute ellipsoid suspension will be calculated, analysing its dependence on the wave frequency and amplitude. In § 4 the merits and limitations of a creeping flow approach to modelling the frazil ice dynamics will be discussed. In § 5, using a differential scheme, the results will be extrapolated from the dilute limit, and will be compared with available data from wave-tank experiments. Section 6 will be devoted to conclusions.

2. Orientation of a disk-like particle in the velocity field of a deep-water gravity wave

We consider a dilute suspension of rigid oblate axisymmetric ellipsoids, supposed small enough that inertia be negligible at the particle scale. We also suppose that the particles are free of external forces or torques and that the suspension is so dilute that the effects of mutual interaction among particles are negligible. In this dilute limit, the rheological properties of the suspension will change from the response of a single particle to the time-dependent wave flow.

In order to represent the wave flow, we introduce a reference frame with the origin at the water surface, the x_1-axis along the direction of propagation of the wave and the x_2-axis pointing vertically towards the sea bottom. Using the hypothesis of small-amplitude inviscid waves in infinitely deep water, we obtain the following velocity field:

$$\left.\begin{aligned} U_1 &= \widetilde{U}\exp(-kx_2)\sin(kx_1-\omega t),\\ U_2 &= \widetilde{U}\exp(-kx_2)\cos(kx_1-\omega t),\end{aligned}\right\} \tag{2.1}$$

where $\tilde{U}$ is a typical value for the fluid velocity in the wave field.

The orientation dynamics in the presence of fore–aft symmetry will in turn be determined by the balance between the strain rate $\boldsymbol{E}$ and the vorticity $\boldsymbol{\Omega}$ of the wave at the particle position, again provided the particle is sufficiently small to allow linearization of the wave field on its scale. In the case of a revolution ellipsoid, with symmetry axis identified by the versor $\boldsymbol{p}$, the orientation dynamics will be described by the Jeffery equation:

$$\dot{\boldsymbol{p}} = \boldsymbol{\Omega}\cdot\boldsymbol{p} + G[\boldsymbol{E}\cdot\boldsymbol{p} - (\boldsymbol{p}\cdot\boldsymbol{E}\cdot\boldsymbol{p})\boldsymbol{p}] + O((ka)^2) \tag{2.2}$$

where G is the ellipsoid eccentricity defined in terms of the particle aspect ratio $r = a/b$, where a and b are respectively along and perpendicular to the symmetry axis, by means of the relation

$$G = \frac{r^2-1}{r^2+1}.$$

For a disk-like particle we have clearly $r \ll 1$ and $G \simeq -1$. For small-amplitude waves, the particle displacement will be small with respect to k^{-1} and we can approximate the instantaneous value of the strain felt by the particle by its value measured at the initial position $\boldsymbol{x}$. Furthermore, for linearized waves, the induced velocity field is confined within a region whose thickness is of the order of the wave amplitude (defined as the valley to crest semi-height): $\mathscr{A} \ll k^{-1}$. We can then approximate $\exp(-kx_2) = 1$. From (2.1) we find easily the expression for the strain rate:

$$\boldsymbol{E} = k\widetilde{U}\begin{pmatrix} \cos(kx_1-\omega t) & -\sin(kx_1-\omega t)\\ -\sin(kx_1-\omega t) & -\cos(kx_1-\omega t)\end{pmatrix}, \tag{2.3}$$

while the vorticity $\boldsymbol{\Omega}$ is identically zero thanks to the potential flow nature of the inviscid wave field. Equation (2.3) describes a strain field rotating with frequency $\omega/2$ around the x_3-axis. Changing variables to a reference frame rotating with the strain, the time dependence in $\boldsymbol{E}$ disappears and a non-zero vorticity is produced:

$$\bar{\boldsymbol{\Omega}} = \frac{\omega}{2}\begin{pmatrix} 0 & 1\\ -1 & 0\end{pmatrix} \tag{2.4}$$

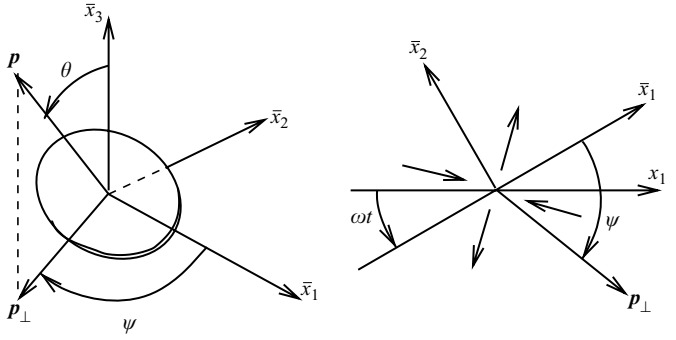

FIGURE 1. Orientation of an ellipsoidal particle in a strain field rotating with angular velocity ω with respect to the laboratory (x_1-axis). For $0 \leqslant \hat{\omega} \leqslant 1$ the symmetry axis $\boldsymbol{p}$ is confined to the strain plane x_1x_2. For $\hat{\omega} \to 0$, alignment with the strain instantaneous compressive direction $\psi = -\pi/4$ occurs. For $0 < \hat{\omega} \leqslant 1$, the symmetry axis of the particles lags behind by a constant angle ψ, with $\psi = -\pi/2$ for $\hat{\omega} = 1$. For $\hat{\omega} > 1$ no stationary solution for ψ exists, corresponding to the particle being unable to follow the rotating strain.

(we identify components in the rotating frame with an overbar). For each value of x_1, we choose the new variables in such a way that the strain rate is

$$\bar{\boldsymbol{E}} = k\widetilde{U} \begin{pmatrix} 0 & 1 \\ 1 & 0 \end{pmatrix}, \tag{2.5}$$

corresponding to the strain expansive direction placed at $\pi/4$ with respect to the rotating $\bar{x}_1$-axis. Introducing polar coordinates (see figure 1), and normalizing time and vorticity with the strain strength $e = k\widetilde{U}$, Jeffery's equation (2.2) leads to the following system of equations:

$$\left.\begin{aligned} \dot{\psi} &= -\hat{\omega} - \cos 2\psi, \\ \dot{\theta} &= -\tfrac{1}{2} \sin 2\theta \sin 2\psi, \end{aligned}\right\} \tag{2.6}$$

where $\hat{\omega} = -\omega/2Ge$ and $\dot{f} = \mathrm{d}f/\mathrm{d}\hat{t}$, $\hat{t} = -Get$. For $\hat{\omega} < 1$,this system of equations has equilibrium solutions $(\psi, \theta) = \frac{1}{2}(\cos^{-1}\hat{\omega} - n\pi, m\pi)$. Of these, only the one

$$\psi = \frac{1}{2}\cos^{-1}\hat{\omega} - \frac{\pi}{2} + n\pi, \quad \theta = \frac{\pi}{2} + n\pi \tag{2.7}$$

is stable and is approached in a time $\sim e^{-1}$. For $\hat{\omega} > 1$, instead, choosing the time so that $\psi(0) = 0$, we have the trajectories:

$$\left.\begin{aligned} \tan\psi(\hat{t}) &= -\left(\frac{\hat{\omega}+1}{\hat{\omega}-1}\right)^{1/2} \tan[(\hat{\omega}^2-1)^{1/2}\hat{t}], \\ \tan\theta(\hat{t}) &= \left(\frac{\hat{\omega}+1}{\hat{\omega}+\cos 2\psi(\hat{t})}\right)^{1/2} \tan\theta(0). \end{aligned}\right\} \tag{2.8}$$

We thus have a high strain regime in which, as illustrated in figure 1, the particles in suspension are all aligned with the local strain and rotate in a coherent fashion, and a low strain regime in which the particles do not rotate, but rather they oscillate around their natural orientation. As it is easy to see from (2.8), the transition from the low to the high strain regime is characterized by the particle spending an increasing amount of time, as $\hat{\omega} \to 1$, near $(-\pi/2, \pi/2)$. This corresponds to the rotation period

of the particle $(\hat{\omega}^2 - 1)^{-1/2}$ (always measured in the rotating frame) going to infinity, as $\psi = -\pi/2$ becomes a fixed point for the system.

The linearized gravity wave theory allows us to write $e = k\widetilde{U}$ in terms of the wave amplitude $\mathscr{A}$ defined as the valley to crest semi-height, the gravitational acceleration g and the wave frequency ω, starting from the dispersion relation:

$$k = \frac{\omega^2}{g} \tag{2.9}$$

and the expression for the typical wave velocity value:

$$\widetilde{U} = \mathscr{A}\omega. \tag{2.10}$$

This leads to the expression for the strain strength e in the small-r regime corresponding to $G = -1$: $e = \mathscr{A}\omega^3/g$ and to the condition for the existence of equilibrium:

$$\omega \geqslant \sqrt{\frac{g}{2\mathscr{A}}}. \tag{2.11}$$

We thus see that in the case of gravity waves, the aligned particle case corresponds to a high-frequency (or small-wavelength) limit. The same transition is observed experimentally in the case of grease ice (see Martin & Kauffman 1981, pp. 307, 308), with the crossover frequency at $\omega \simeq \sqrt{0.35g/\mathscr{A}}$.

3. The bulk stress and the effective viscosity of the fluid–particle mixture

The bulk stress of a dilute suspension of axisymmetric ellipsoidal particles is given by the law (Leal & Hinch 1972; Hinch & Leal 1975)

$$\boldsymbol{\sigma} = P\boldsymbol{I} + 2\mu\boldsymbol{E} + 2\mu\phi\{2A\langle \boldsymbol{pppp}\rangle : \boldsymbol{E} + 2B[\langle \boldsymbol{pp}\rangle \cdot \boldsymbol{E} + \boldsymbol{E} \cdot \langle \boldsymbol{pp}\rangle] + C\boldsymbol{E} + F\langle \boldsymbol{pp}\rangle \cdot \boldsymbol{D}\} \tag{3.1}$$

where μ is the dynamic viscosity of the pure fluid, P is the pressure, ϕ is the volume fraction of the particles, A, B, C, F are dimensionless shape coefficients and $\boldsymbol{D}$ is a term that takes into account Brownian motion effects. It is an open question whether other effects, such as interaction with other particles, could be modelled by a noise term. The presence of this term, independently of its amplitude, guarantees that the memory of any initial particle orientation, including unstable equilibrium points, is lost and a statistical equilibrium state, in an $O(D^{-1})$ time, is eventually reached.

Following Leal & Hinch (1972), we shall consider the small noise limit in which D^{-1} is much longer than the other timescales of the process, which are given in dimensionless form by $(\hat{\omega}^2 - 1)^{-1/2}$. Over these timescales, the evolution of the process will be therefore, to lowest order, that of the unperturbed system.

The second and fourth moments of $\boldsymbol{p}$ are calculated functions of the PDF (probability density function) for the particle orientation $\rho(\theta, \psi, t)$. The A, B, C coefficients may be obtained from Jeffery (1922), in terms of the following elliptic integrals:

$$\alpha' = \int_0^\infty \frac{\mathrm{d}\lambda}{(b^2+\lambda)^3\sqrt{a^2+\lambda}}, \qquad \alpha'' = \int_0^\infty \frac{\lambda\,\mathrm{d}\lambda}{(b^2+\lambda)^3\sqrt{a^2+\lambda}},$$

$$\beta' = \int_0^\infty \frac{\mathrm{d}\lambda}{(b^2+\lambda)^2(a^2+\lambda)\sqrt{a^2+\lambda}}, \qquad \beta'' = \int_0^\infty \frac{\lambda\,\mathrm{d}\lambda}{(b^2+\lambda)^2(a^2+\lambda)\sqrt{a^2+\lambda}},$$

where a and b identify the ellipsoid semi-axes parallel and perpendicular, respectively, to the symmetry axis. More precisely

$$A = \frac{\alpha''}{2b^2\alpha'\beta''} + \frac{1}{2b^2\alpha'} - \frac{2}{\beta'(a^2+b^2)}, \quad B = \frac{1}{\beta'(a^2+b^2)} - \frac{1}{b^2\alpha'}, \quad C = \frac{1}{b^2\alpha'}.$$

In the case of disk-like ($r \ll 1$) particles, disregarding $O(r)$ terms gives

$$A = \frac{5}{3\pi r} + \frac{104}{9\pi^2} - 1, \quad B = -\frac{4}{3\pi r} - \frac{64}{9\pi^2} + \frac{1}{2}, \quad C = \frac{8}{3\pi r} + \frac{128}{9\pi^2}. \tag{3.2}$$

Notice that this value of C differs at subleading order $O(1)$ from the one in Leal & Hinch (1972). As seen in the previous section, two orientation dynamics regimes are possible and these affect the value of the angular averages entering (3.1). We consider in detail the two regimes below.

From the stress $\boldsymbol{\sigma}$, it is possible to calculate an effective viscosity $\bar{\mu}$ in terms of the viscous dissipation in the suspension, exactly as is done with spherical particles:

$$\bar{\mu} = \frac{1}{2}\frac{\boldsymbol{\sigma} : \boldsymbol{E}}{\boldsymbol{E} : \boldsymbol{E}} := (1 + K\phi)\mu \tag{3.3}$$

where K is called the reduced viscosity of the suspension.

3.1. *Preferential orientation regimes:* $0 \leqslant \hat{\omega} \leqslant 1$

In this regime, after a relaxation time $\sim e^{-1}$, all particles tend to align, in the rotating frame, in the direction identified by (2.7). For small diffusivities, the variance of the distribution around these fixed points will be D/e. As already mentioned, this state of affairs corresponds, in the laboratory frame, to the particles rotating in a coherent fashion with the wave field. The fourth- and second-order tensors $\langle \boldsymbol{pppp} \rangle$ and $\langle \boldsymbol{pp} \rangle$ have a simpler form in the rotating reference frame with the $\bar{x}_1$-axis along $\boldsymbol{p}$. In this new frame of reference, the rate of strain tensor $\boldsymbol{E}$ takes the following form:

$$\bar{\boldsymbol{E}} = e \begin{pmatrix} -\sqrt{1-\hat{\omega}^2} & \hat{\omega} \\ \hat{\omega} & \sqrt{1-\hat{\omega}^2} \end{pmatrix}$$

while the $\langle \boldsymbol{pppp} \rangle$ and $\langle \boldsymbol{pp} \rangle$ tensors are

$$\langle \bar{p}_i \bar{p}_j \bar{p}_k \bar{p}_l \rangle = \delta_{1i}\delta_{1j}\delta_{1k}\delta_{1l}, \quad \langle \bar{p}_i \bar{p}_j \rangle = \delta_{1i}\delta_{1j}$$

where δ_{ij} is the Kronecker delta. Substituting into (3.1) and (3.3), the reduced viscosity coefficient K, is easily obtained:

$$K = A(1-\hat{\omega}^2) + 2B + C. \tag{3.4}$$

From (3.4), the dominant $O(r^{-1})$ contribution to the viscosity is the $\hat{\omega}$-dependent contribution proportional to A, while $2B + C = 1 + O(r)$. For this reason, the reduced viscosity K is characterized by a minimum at the crossover $\hat{\omega} = 1$, at which $K \simeq 1$ (compare with the spherical particle value $K = 5/2$ (Landau & Lifshitz 1959)).

3.2. *Continuously rotating regime:* $\hat{\omega} \geqslant 1$

In the laboratory frame this regime corresponds to the particle oscillating around its initial orientation, while slowly diffusing with respect to angle, under the effect of Brownian couples. In the rotating frame, the problem can be mapped to that of an ellipsoid in a plane shear: the equation of motion for a particle in the rotating frame

(2.8) is identical to that of a particle with aspect ratio

$$s = \left(\frac{\hat{\omega}-1}{\hat{\omega}+1}\right)^{1/2} \tag{3.5}$$

in a plane shear $\omega = 2e$. The equilibrium distribution of an ensemble of particles whose orientation dynamics is described by (2.6), in the presence of an isotropic Brownian couple, is then obtained from the theory of Leal & Hinch (1972), whose main results are reported below.

The particle orientation is identified by the variables $\hat{t}$ and c where $\hat{t}$ is defined by the first of (2.8) and gives the normalized time needed, on the Jeffery orbit starting from the current values of θ and ψ, to go from $\psi = 0$ to the current value of ψ, while c obeys

$$c = \left(\frac{\hat{\omega}+\cos 2\psi}{\hat{\omega}-1}\right)^{1/2} \tan\theta. \tag{3.6}$$

Thus, $\tan^{-1} c$ is the value of θ at $\psi = \pi/2$, and identifies the Jeffery orbit.

In these variables, the orientation PDF can be decomposed as

$$\rho(c, \hat{t}) = \rho(\hat{t}|c)\rho(c). \tag{3.7}$$

The marginal PDF $\rho(c)$ is given by

$$\rho(c) = \text{const.}\, c[(H_4c^4 + H_2c^2 + H_0)F]^{-3/4} \tag{3.8}$$

where

$$H_4 = s^2 + 1, \quad H_2 = \frac{1}{4}s^2 + \frac{7}{2} + \frac{1}{4s^2}, \quad H_0 = \frac{1}{s^2}(s^2+1)$$

and

$$F = \begin{cases} \left[\dfrac{2H_4c^2 + H_2 - S}{2H_4c^2 + H_2 + S}\right]^{(4-H_2)/S}, & H_2^2 > 4H_4H_0, \\ \exp\left[\dfrac{2(H_2-4)}{2H_4c^2 + H_2}\right], & H_2^2 = 4H_4H_0, \\ \exp[2S^{-1}(H_2-4)\tan^{-1} S^{-1}(2H_4c^2 + H_2)], & H_2^2 < 4H_4H_0, \end{cases} \tag{3.9}$$

where $S = |H_2^2 - 4H_4H_0|^{1/2}$.

The PDF $\rho(c)$ is all that is needed, since the averages along the orbits of the tensors $\boldsymbol{pp}$ and $\boldsymbol{pppp}$ are already available (Jeffery 1922). In fact, from (3.3), the reduced viscosity can be written as

$$K = A\langle \sin^4\theta \sin^2 2\psi\rangle + 2B\langle \sin^2\theta\rangle + C, \tag{3.10}$$

but, from Jeffery (1922):

$$\langle \sin^4\theta \sin^2 2\psi | c\rangle = \frac{2s^2}{(s^2-1)^2}\left[\frac{c^2(s^2+1)+2}{[(c^2s^2+1)(c^2+1)]^{1/2}} - 2\right]$$

and

$$\langle \sin^2\theta | c\rangle = 1 - \frac{1}{[(c^2s^2+1)(c^2+1)]^{1/2}}.$$

Completing the averages by means of (3.8), leads to behaviours for $\langle \sin^4\theta \sin^2 2\psi\rangle$ and $\langle \sin^2\theta\rangle$ shown in figure 2. Substituting into (3.10) with the expressions for the

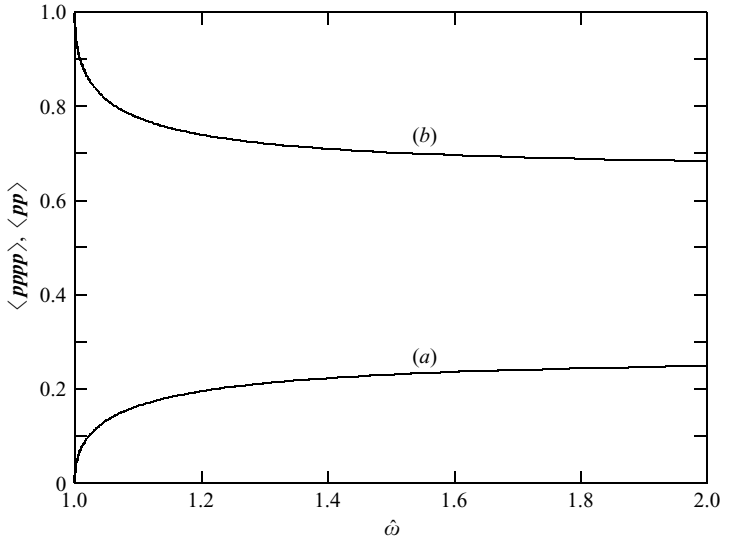

FIGURE 2. Plot of $\langle \sin^4\theta \sin^2 2\psi \rangle$ (a) and $\langle \sin^2\theta \rangle$ (b) vs. $\hat{\omega}$ in the low strain range.

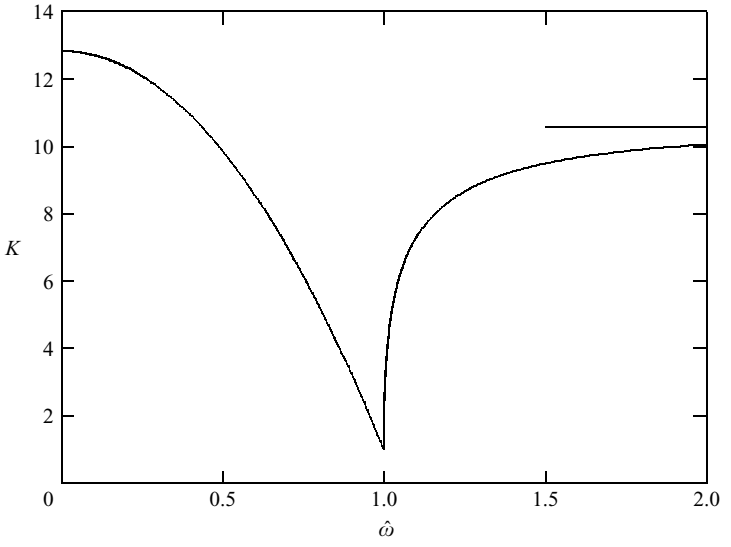

FIGURE 3. Reduced viscosity vs. normalized frequency $\hat{\omega} \simeq \omega/2e$ for a disk-like particle with aspect ratio $r = 0.045$. From $\hat{\omega} \propto \omega^{-2}$, the long-wave regime corresponding to random particle orientation, occurs for $\hat{\omega} > 1$ and the short-wave one, corresponding to coherent motion, for $\hat{\omega} < 1$. The horizontal line to the right gives the asymptotic value $K(\hat{\omega} \to \infty)$.

coefficients A, B and C provided by (3.2), allows one to determine the reduced viscosity of a dilute suspension of ellipsoidal particles, for arbitrary values of the aspect ratio r and of the reduced frequency $\hat{\omega}$. As in the continuously rotating regime, we see that the effective viscosity grows away from the crossover at $\hat{\omega} = 1$, with the dip becoming more pronounced as the aspect ratio r goes to zero. This is illustrated in figure 3, in the case of a disk-like particle with a value of the aspect ratio in the range characteristic for frazil ice. Notice that the asymptotic regime of random particle

orientation $\rho(\theta, \psi) = \sin\theta/4\pi$, leading to the expression for the reduced viscosity (Phan-Thien & Pham 2000)

$$K = \frac{4}{15}A + \frac{4}{3}B + C,$$

has already been obtained for relatively small values of the reduced frequency $\hat{\omega} \simeq 2$.

We remark that, using the values C given in Leal & Hinch (1972), would have produced an unphysical negative value of the reduced viscosity K at the crossover.

4. Grease ice

The analysis carried out so far assumed a dilute regime, which is very different from the conditions typical of grease ice. Furthermore, the analysis assumed creeping flow conditions, which may be problematic for millimetre size particles. As regards the first issue, the differential scheme, originally proposed by Bruggeman (1935), provides an analytical method to generalize the well-known Einstein formula for the effective viscosity of dilute suspensions to finite concentrations (Brinkman 1952; Roscoe 1952). More recently, the differential scheme has been exploited to study the viscosity problems related to randomly oriented spheroidal inclusions in viscous fluids (Phan-Thien & Pham 2000).

The basic idea is to calculate the increment of effective viscosity that is obtained by adding a volume Δv of particles to a volume v_0 of suspension already containing a fraction v/v_0 of particles. Let us indicate with $\nu = \mu/\rho_w$ the kinematic viscosity of the solvent and with $\bar{\nu} \simeq \bar{\mu}/\rho_w$ the same quantity referred to the suspension, with ρ_w the density of the solvent, assumed approximately equal to that of the suspension. The increment in volume fraction is

$$\Delta\phi = \frac{v + \Delta v}{v_0 + \Delta v} - \frac{v}{v_0} \simeq (1 - v/v_0)\Delta v/v_0 = (1 - \phi)\Delta v/v_0$$

while the increment in effective viscosity $\bar{\nu}$ will be

$$\Delta\bar{\nu} = \frac{K\bar{\nu}\Delta v}{v_0 + \Delta v}$$

leading to the differential equation

$$\mathrm{d}\bar{\nu}/\mathrm{d}\phi = K\bar{\nu}/(1 - \phi), \qquad \bar{\nu}(0) = \nu. \tag{4.1}$$

The differential scheme assumes implicitly that viscosity renormalization is the only effect of particle inclusion, which is strictly true only when the particle orientation distribution and consequently the viscosity tensor are isotropic. In the opposite limit $\hat{\omega} \leqslant 1$, the theory of Sundararajakumar *et al.* (1994) could be applied.

In the case of microscopic (Stokesian) particles, (4.1) could be integrated from the initial condition (corresponding to pure solvent) to the final concentration ϕ, using for K the constant value obtained from (3.2), (3.4), (3.10) and the data in figure 2. In this case, the solution would be

$$\bar{\nu}(\phi) = \nu(1 - \phi)^{-K}. \tag{4.2}$$

(This equation allows a maximum packing fraction $\phi_{max} = 1$ which is above the real value $\phi_{max} \simeq \pi/4$ appropriate for stacked disks.) In the case of frazil particles, in the integration of (4.1), there is an initial range of values of ϕ in which $\bar{\nu}(\phi)$ is likely to be too small for the creeping flow approximation to apply; in that range, the

stress coefficients and K will probably differ from their zero-Reynolds-number limit. Hence $K = K(\phi)$ and (4.2) will provide at most an order of magnitude estimate for the effective viscosity of grease ice.

To determine the importance of these effects, let us consider an individual ice platelet in a suspension of effective viscosity $\bar{\nu}$. Creeping flow conditions require stationarity and small particle Reynolds numbers. Introducing the effective Stokes time $\bar{\tau}_S \sim b^2/\bar{\nu}$:

$$\omega\bar{\tau}_S = \frac{\omega b^2}{\bar{\nu}} \ll 1, \qquad Re_p = \frac{eb^2}{\bar{\nu}} = \omega\bar{\tau}_S k\mathscr{A} \ll 1, \tag{4.3}$$

where $e = k\widetilde{U}$ is the strain strength. In the case of a dilute suspension, $\bar{\nu} = \nu \simeq 0.01\,\mathrm{cm^2\,s^{-1}}$; taking for the particle radius the value $b \sim 0.1\,\mathrm{cm}$, we would obtain from (2.9), (2.10), values for $\omega\bar{\tau}_S$ ranging from 1 in open sea, to 10 in laboratory conditions. As regards the condition on Re_p, this is satisfied in open sea, where $k\mathscr{A}$ is of the order of a few hundredths, but only marginally in the laboratory, where $k\mathscr{A} \sim 0.3$ (Martin & Kauffman 1981). Clearly, the conditions of (4.3) will be satisfied in the case where the suspending medium is grease ice, when $\bar{\mu} \sim 10^2\,\mathrm{cm^2\,s^{-1}}$. This has the consequence, in particular, that the results on the orientation dynamics of § 2 are expected to remain valid overall.

In the dilute case, the non-satisfaction of the conditions in (4.3) has another consequence, namely inertia will cause relative particle–fluid motions and additional dissipation in the suspension. We can obtain an estimate of this effect. The particle velocity $\boldsymbol{V}$, subtracted from the contribution from the buoyancy-produced drift, will obey an equation in the form

$$\left(\frac{\mathrm{d}}{\mathrm{d}t} + \frac{1}{\bar{\tau}_S}\boldsymbol{\Pi}\cdot\right)(\boldsymbol{V} - \boldsymbol{U}) \simeq \epsilon r\frac{\mathrm{d}\boldsymbol{V}}{\mathrm{d}t} + \frac{1}{\bar{\tau}_S}\boldsymbol{F}\cdot\boldsymbol{U} + \boldsymbol{f} \tag{4.4}$$

with $\epsilon = 1 - \rho_p/\rho_w \simeq 0.1$, ρ_p indicating the ice density, $\boldsymbol{F} = O((kb)^2)$ accounting for the Faxen force and $\boldsymbol{\Pi}$ the non-dimensionalized resistance tensor, whose components are $O(1)$ for the range of $\omega\bar{\tau}_S$ we are interested in (Zhang & Stone 1998). The term $\boldsymbol{f}$ is a noise contribution accounting for collision effects with other particles and Brownian motion. All inertia effects in the wave flow and from the particle relative motion are in first instance neglected.

The contribution to relative motion from collisions is important in bubbly flows (Kang *et al.* 1997), but can be shown to be negligible in the present case due to the regime $Re_p < 1$. Let us show this. We can estimate the noise amplitude in a kinetic approach by introducing first the collision frequency τ_c^{-1}:

$$\tau_c^{-1} \sim n\Delta V b^2 = \frac{\phi\Delta V}{a}$$

where $n = \phi/ab^2$ is the numerical density of the particles, $\Delta V \sim |\boldsymbol{V} - \boldsymbol{U}|$ estimates the typical collision velocity and b^2 estimates the collision cross-section. Collisions will be important provided $\tau_c < \bar{\tau}_S$; in this case, taking the noise as uncorrelated $\langle f(t)f(t')\rangle \sim D\delta(t - t')$, we would have for its amplitude

$$D \sim \Delta V^2\tau_c \sim \frac{a\Delta V}{\phi}.$$

From (4.4), considering f dominant over the other terms on the right-hand side, we obtain the estimate for the velocity $\Delta V \sim e(D\bar{\tau}_S)^{1/2}$; this is the velocity difference in the wave field sampled by the diffusing particle in the relaxation time $\bar{\tau}_S$. Substituting

$\hat{\omega}$	ϕ	$\omega\,(\mathrm{s}^{-1})$	$\mathscr{A}\,(\mathrm{cm})$	$h\,(\mathrm{cm})$	$q\,(\mathrm{m}^{-1})$	$\bar{\nu}\,(\mathrm{cm\,s}^{-2})$	K
1.4–1.5	0.30–0.34	14.9	1.45–1.55	6–7	5.3 ± 0.4	243–250	18.7 ± 0.2
1.3–1.4	0.29–0.34	14.9	1.6–1.7	7–8	6.6 ± 0.6	353–361	19.7 ± 0.3
1.2–1.3	0.28–0.32	14.9	1.7–1.8	8–9	5.8 ± 0.5	275–280	20.3 ± 0.2
1.2–1.5	0.28–0.34	14.9	1.5–1.8	7–8.5	1.6 ± 0.1	587–603	15.6 ± 0.1
1.2–1.5	0.34–0.35	14.9	1.5–1.8	8.5–10	7.5 ± 0.5	454–463	18.6 ± 0.3
1.4–1.4	0.35–0.44	10.7	3.0–3.1	14–16	3.5 ± 0.2	1010–1029	17.2 ± 0.2

TABLE 1. Experimental parameters.

the expressions for D and $\bar{\tau}_S$, we find

$$\Delta V \sim \frac{ab^2e^2}{\phi\bar{\nu}}$$

and substituting in the expression for τ_c and comparing with $\bar{\tau}_S$, we see that the condition $\bar{\tau}_S > \tau_c$ is equivalent to $Re_p > 1$. Interparticle collisions can then be neglected.

Passing to the contribution to $\boldsymbol{V} - \boldsymbol{U}$ from direct acceleration by the wave field, we see that, for waves in both laboratory ($k \sim 10^{-1}\,\mathrm{cm}^{-1}$) and open sea ($k \sim 10^{-3}\,\mathrm{cm}^{-1}$) conditions, the Faxen force can be disregarded. Neglecting the noise in (4.4), we obtain in this limit:

$$|\boldsymbol{V} - \boldsymbol{U}| \sim \epsilon r \widetilde{U} \min(1, \omega\bar{\tau}_S).$$

The dissipation produced by a single particle due to its translation relative to the fluid can be estimated from the product of the drag force in (4.4) and $|\boldsymbol{V} - \boldsymbol{U}|$ as $\rho_w b^3 \Pi |\boldsymbol{V} - \boldsymbol{U}|^2/\bar{\tau}_S$. The contribution from relative particle fluid rotation will be smaller by a factor kb. The dissipation per unit volume will be therefore

$$W_{tr} \sim \bar{\mu}\phi r \left(\frac{\epsilon\widetilde{U}}{b}\right)^2 \min(1, \omega\bar{\tau}_S)^2,$$

to be compared with the viscous dissipation $W_v = \bar{\mu}(k\widetilde{U})^2$. We thus see that the contribution to dissipation from relative particle–fluid motion is dominant in the dilute case, but decreases with $1/\bar{\mu}$ when $\omega\bar{\tau}_S < 1$. Taking values for $\bar{\mu}$ in the range of hundreds, and $\phi \sim 0.3$, as observed in grease ice (see also table 1), we see that the contribution to dissipation from relative particle-fluid motion is negligible, with the ratio W_{tr}/W_v varying from 10^{-4} in the open sea to 10^{-8} in the laboratory.

In conclusion, inertia and non-stationarity are likely to contribute to the effective value of the grease ice effective viscosity, but do not affect the frazil orientation dynamics described in § 2. It is also confirmed that the dominant contribution to dissipation and to the effective viscosity is the particle-induced stress and not particle–fluid motions.

5. Comparison with experiments

We have compared the order of magnitude estimate for the effective viscosity, provided by (4.2), with the wave tank data of Martin & Kauffman (1981). In their experiment, concentrated suspensions of grease ice with thicknesses varying from 7 to 15 cm and volume fraction ϕ between 0.28 to 0.44, were allowed to grow in a 2 m long tank previously filled with saline water to a depth of 41 cm. We selected those measurements relevant to propagation of deep waves in a grease ice layer according

to the criterion $kh \geqslant \pi/2$, where k is the open-water wavenumber and h is the ice layer thickness (Phillips 1966). The relevant parameters of the experimental data we are considering are listed in table 1. As already discussed, the differential scheme assumes an isotropic suspension. Comparing the values of $\hat{\omega}$ in table 1 with figure 3, we see that the data fall in the range where this assumption holds. Grease ice effective viscosities were estimated from the measured spatial attenuation rate $q = -\mathscr{A}^{-1}\mathrm{d}\mathscr{A}/\mathrm{d}x_1$ using a two-layer viscous fluid wave propagation model (De Carolis & Desiderio 2002). The model can be inverted to obtain the effective viscosity $\bar{\nu}$ of the grease ice from the experimentally observed values of the wave frequency ω, the attenuation rate q and the thickness h and volume fraction ϕ of the frazil. The reduced viscosity K can then be determined from (4.2) in order to estimate the corresponding particle aspect ratio by means of (3.2), (3.4), (3.10) and the data in figure 2. From the data in table 1, we obtain the estimate: $r \sim 2 \times 10^{-2}$, to be compared with the individual observation presented in Martin & Kauffman (1981) of a disk diameter of 0.1 cm and thickness of 1–10 μm (see their figure 11). The corresponding range of variability for frazil ice in a geophysical environment is 0.1–0.4 cm in diameter and 1–100 μm in thickness (Kivisild 1970), corresponding to $0.25\times10^{-4} < r < 0.1$.

6. Conclusions

We have obtained predictions of the effective viscosity dependence of a suspension of disk-like particles, in the velocity field of deep-water waves, of the aspect ratio and the concentration of the particles. A key parameter appears to be, in the dilute limit, the relative strength of the wave field strain, which parameterizes the wave amplitude, and the wave frequency. For high-amplitude waves, collective alignment of the particles in suspension with the wave field is possible, with the crossover to this regime signalled by a deep minimum in the effective viscosity. This minimum is lower than the effective viscosity in the case of spherical particles and can be smaller, by orders of magnitude, than the value of the effective viscosity of a disk-like particle suspension away from the crossover.

An interesting question is whether these behaviours are preserved away from the deep-water wave regime we have considered in this paper. For shallow-water waves, a rotating system in which the flow becomes time-independent no longer exists, and irregular behaviours of the kind described in Szeri *et al.* (1992) become possible.

Some of these results extrapolate from the dilute limit to the case of grease ice, in particular the presence of a crossover to coherent alignment of the particles for large-amplitude waves (Martin & Kauffman 1981). As regards the effective viscosity of the grease ice, this appears to be dominated by the stress contribution from the individual particles rather than from momentum transport from relative particle–fluid motion. This is in contrast to other situations, e.g. bubble-laden flows (Kang *et al.* 1997), in which the second is the dominant effect. A creeping-flow-based calculation of the effective viscosity, aided by the use of a differential scheme, to deal with the high concentration regime, leads to results consistent with experiments.

This work was supported by the Commission of the European Communities under contract EVK2-2000-00544 of the Environment and Climate Programme. The authors would like to thank Professor G. Spiga for valuable comments and stimulating discussions.

REFERENCES

Bretherton, F. P. 1962 The motion of rigid particles in a shear flow at low Reynolds number. *J. Fluid Mech.* **14**, 280–304.

Brinkman, H. C. 1952 The viscosity of concentrated suspensions and solutions. *J. Chem. Phys.* **20**, 571.

Bruggeman, D. A. G. 1935 Berechnung verschiedener physkilisher konstante von heterogene substazen. *Ann. Physik* **24**, 636–679.

De Carolis, G. & Desiderio, D. 2002 Dispersion and attenuation of gravity waves in ice: a two-layer viscous fluid model with experimental data validation. *Phys. Lett.* A **305**, 399–412.

Hinch, E. J. & Leal, L. G. 1975 Constitutive equations in suspension mechanics. Part 2. Approximate forms of a suspension of rigid particles affected by Brownian rotations. *J. Fluid Mech.* **76**, 187–208.

Jeffery, G. B. 1922 The motion of ellipsoidal particles immersed in a viscous fluid. *Proc. R. Soc. Lond.* A **102**, 161–179.

Kang, S.-Y., Sangani, A. S., Tsao, H.-K. & Koch, D. L. 1997 Rheology of dense bubble suspensions. *Phys. Fluids* **9**, 1540–1561.

Keller, J. 1998 Gravity waves on ice-covered water. *J. Geophys. Res.* **103**, 7663–7669.

Kivisild, H. R. 1970 River and lake ice terminology. *Intl Assoc. Hydraul. Res.* Paper 1.0, 14 pp.

Landau, L. D & Lifshitz, E. M. 1959 *Fluid Mechanics*. Pergamon.

Leal, L. G. & Hinch, E. J. 1972 The effect of weak Brownian rotations on particles in shear flows. *J. Fluid Mech.* **46**, 685–703.

Martin, S. & Kauffman, P. 1981 A field and laboratory study of wave damping by grease ice. *J. Glaciol.* **96**, 283–313.

Newyear, K. & Martin, S. 1997 A comparison of theory and laboratory measurements of wave propagation and attenuation in grease ice. *J. Geophys. Res.* **102**, 25091–25099.

Newyear, K. & Martin, S. 1999 Comparison of laboratory data with a viscous two-layer model of wave propagation in grease ice. *J. Geophys. Res.* **104**, 7837–7840.

Phan-Thien, N. & Pham, D. C. 2000 Differential multiphase models for polydispersed spheroidal inclusions: thermal conductivity and effective viscosity. *Intl J. Engng Sci.* **38**, 73–88.

Phillips, O. M. 1966 *Dynamics of the Upper Ocean*. Cambridge University Press.

Roscoe, R. 1952 The viscosity of suspensions of rigid spheres. *Br. J. Appl. Phys.* **3**, 267–269.

Sundararajakumar, R. R., Koch, D. L. & Shaqfeh, E. S. G. 1994 The extensional viscosity and effective thermal conductivity of a disersion of aligned disks. *Phys. Fluids* **6**, 1955–1962.

Szeri, A. J., Milliken, W. J. & Leal, L. G. 1992 Rigid particles suspended in time-dependent flows: irregular versus regular motion, disorder versus order. *J. Fluid Mech.* **237**, 33–56.

Taylor, G. I. 1923 The motion of ellipsoidal particles in a viscous fluid. *Proc. R. Soc. Lond.* A **103**, 58–61.

Wadhams, P. & Holt, B. 1991 Waves in frazil and pancake ice and their detection in Seasat synthetic aperture radar imagery. *J. Geophys. Res.* **96**, 8835–8852.

Zhang, W. & Stone, H. A. 1998 Oscillatory motions of circular disks and nearly spherical particles in viscous flows. *J. Fluid Mech.* **367**, 329–358.